Available online at www.sciencedirect.com
ScienceDirect
Trans. Nonferrous Met. Soc. China 31(2021) 3162−3176
Transactions of Nonferrous Metals Society of China
www.tnmsc.cn

Thermodynamic and kinetic analysis of CrB_2 and VB_2 formation in molten Al−Cr−V−B alloy

A. KHALIQ[1,2], H. T. ALI[3], M. YUSUF[4]

1. Department of Mechanical Engineering, College of Engineering, University of Ha'il, Kingdom of Saudi Arabia;
2. School of Engineering, RMIT University, Melbourne, VIC 3000, Australia;
3. Department of Mechanical Engineering, College of Engineering, Taif University, P. O. Box 11099, Taif 21944, Kingdom of Saudi Arabia;
4. Department of Clinical Pharmacy, College of Pharmacy, Taif University, P. O. Box 11099, Taif 21944, Kingdom of Saudi Arabia

Received 29 August 2020; accepted 28 February 2021

Abstract: Transition metal impurities such as chromium (Cr) and vanadium (V) in solution deteriorate electrical conductivity of smelter grade aluminium (Al). These impurities can be removed from solution via boron treatment in which borides form upon their in-situ reaction with boron (B)-bearing substances. However, Cr removal from smelter grade Al solution is not well understood. A disagreement related to chromium boride (CrB_2) formation in molten Al in the presence of other transition metals (V, Ti, Zr, Fe) by adding Al−B master alloy has been reported in literatures. This study presents an effort to understand the mechanism of Cr removal from Al−0.50%Cr−0.50%V (mass fraction) alloy by adding Al−B (AlB_{12}) master alloy at 1023 K in the Al alloy solution. Results indicate that Cr removal from molten Al−0.50%Cr−0.50%V alloy by forming stable borides cannot be achieved at 1023 K; whereas excess of B in the solution preferentially forms aluminium boride (AlB_2) over CrB_2 during boron treatment of molten Al. The underlying kinetics of V removal from molten Al−0.50%Cr−0.50%V alloy revealed that early reaction stage is controlled by [B]/[V] mass transfer through liquid phase and mass transfer coefficient (k_m) was measured to be 9.6×10^{-4} m/s. The later reaction stage was controlled by [B]/[V] diffusion through boride (VB_2) ring. This study, therefore, advocates to investigate alternative ways to remove Cr from molten Al.

Key words: boron treatment; Al; CrB_2; VB_2; thermodynamics; kinetics

1 Introduction

Aluminium (Al) has emerged as a promising material to replace copper for electrical conductor (EC) applications particularly in the overhead power transmission [1,2]. However, a large number of metallic impurities in smelter grade Al reduce its electrical conductivity [3,4]. Raw materials used for Al production contain numbers of transition metal impurities such as Cr, V, Ti, Zr and Fe. In the Hall−Heroult electrolysis process, raw materials (pitch, petroleum coke and bauxite (Al_2O_3)), cell materials (refractory linings and carbon cathode), and others (furnaces, linings and ladles) are generally considered as primary sources of impurities in Al [5−8]. Impurity content in Al varies from 0 to 0.3 wt.%. In cast-houses, smelter grade Al is treated through a series of refining processes to remove such metallic impurities [9]. The solubility limits of various metals in Al and their effects on the electrical resistivity of Al are shown in Table 1. It is evident from Table 1 that deleterious effect of transition metal impurities can be minimized by

Corresponding author: A. KHALIQ, E-mail: drabdulkhaliq82@gmail.com
DOI: 10.1016/S1003-6326(21)65723-0
1003-6326/© 2021 The Nonferrous Metals Society of China. Published by Elsevier Ltd & Science Press

Table 1 Maximum solubility and influence of various metallic impurities on electrical resistivity of Al at 298 K by 1% addition in Al solution [3]

Element	Max. solubility/wt.%		Resistivity increase with impurities removed from solution/(μΩ·cm)
	In Al	In solution	
Cr	0.77	4.00	0.18
V	0.55	3.58	0.28
Zr	0.28	0.28	0.044
Ti	1.0	2.88	0.12
Ni	0.05	0.81	0.061
Fe	0.052	2.56	0.058

removing them from solution state to stable state (solid phase).

Impurities control is therefore considered to be critical to produce high quality electrical conductors and other electrical products from Al. Key strategies might be as follows.

(1) Impurities control at beginning of the Al production. This includes measures to control impurities in the raw materials (bauxite and petroleum coke). This approach has a limitation as quality of raw material declines with the time [10].

(2) Another strategy is to treat smelter grade Al in cast-house for removal of the impurities coming from primary production process (electrolytic process). In-line fluxing and degassing processes have been developed to remove alkali and alkaline earth metals from molten metals [11]. Reactive impurities (transition metals of Cr, V, Zr, Ti and Fe) are removed by combining them with another element that transforms them into stable solid phase such as borides. Solid inclusions (oxides, nitrides, borides and carbides) are removed by filtration or gravity settling. Various Al refining processes have been reported in Ref. [9].

Generally, transition metal impurities are removed from smelter grade Al by engineering the casting conditions in which these impurities react with boron (B)-bearing substances. This process is well established and known as boron treatment [6,12−15]. In this process, various sources of B such as pure B, aluminium borides (AlB_2) and (AlB_{12}) have been used on a commercial scale [16−20]. Al−Ti−B master alloys containing TiB_2 particles have also been used for grain refinement of Al alloys [20−22]. Transition metal impurities in Al solution react with B and form in-situ borides. These in-situ formed borides are generally stable and do not re-dissolve in Al during their processing at 973−1023 K. Removal of the transition metals from molten Al by adding Al−B master alloys (AlB_2/AlB_{12}) on laboratory and industrial scales has also been thoroughly investigated [23−29]. In these investigations, a combination of thermodynamic modelling and experimental approaches was adopted. However, a critical analysis of thermodynamic predictions under various processing conditions (B content and temperature) provided concrete foundation for various experimental studies. For example, KHALIQ et al [23] investigated the thermodynamics and kinetics of V and zirconium (Zr) removal from molten Al. In their study, Al−1%V−0.721%B ternary alloy analysis revealed that it is feasible both thermodynamically and kinetically, to remove V from molten Al in the form of their stable borides (VB_2). It was also reported that overall reaction between [V] and B/AlB_{12} was sluggish and could be divided into two distinct stages, as shown in Fig. 1 [24]. Early-stage reaction was controlled by [V] mass transfer in the liquid (Al) phase. Stage I was composed of the first 6 min starting from Al−B (AlB_{12}) master alloy addition into molten Al. The [V] mass transfer coefficient was measured to be 2.15×10^{-3} m/s and reaction activation energy was measured to be 25.94 kJ/mol at 1023 K. It was further suggested that Stage II was significantly slower compared to Stage I and was preferentially governed by diffusion of [V] and [B] from VB_2 solid layer. This could be observed by thickening of the reaction product layer (VB_2), as shown in Fig. 1. The calculated reaction rate constant was 1.67×10^{-6} s^{-1} that represents mass transfer through solid phase rather than liquid phase. The Al−0.5%Zr−0.5%V−0.112%B alloy studies [28,29] revealed that kinetics of Zr removal (ZrB_2 formation) was faster compared to V (VB_2 formation) removal from molten Al at 1023 K. Reaction between [B]/AlB_{12} and [Zr]/[V] was incomplete which might be due to undissolved AlB_{12} particles in the Al matrix. It was further noted that compared to VB_2, ZrB_2 preferentially forms in molten Al at 1023 K during boron treatment process.

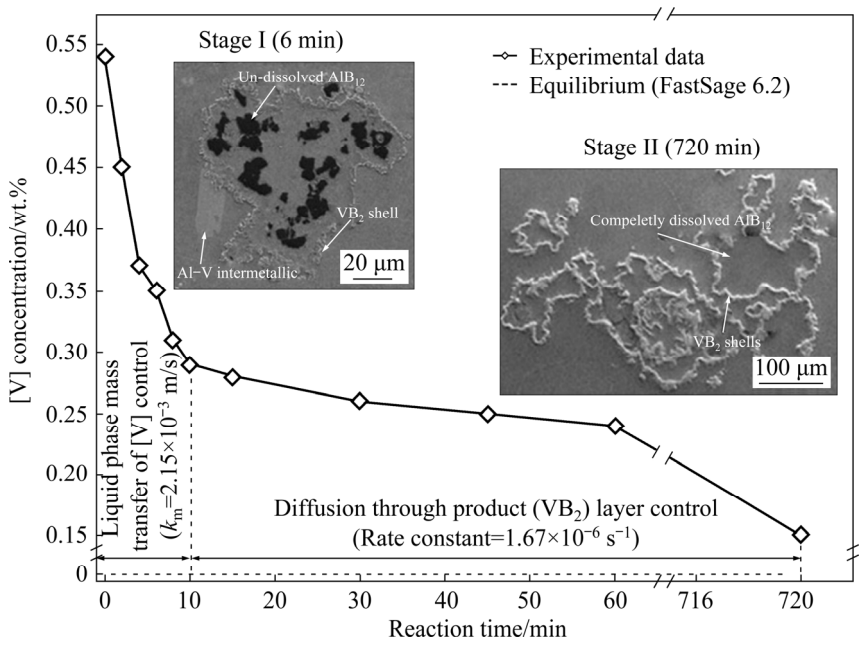

Fig. 1 Mechanism of VB_2 formation in Al−1wt.%V−0.412%B alloy at 1023 K [24]

2 Background of Cr removal from molten Al

Chromium (Cr) removal from molten Al is not well understood to date. There are conflicting observations related to Cr removal in the form of stable CrB_2. DUBE [12] developed a technique to remove Ti and V as complex borides $(V,Ti)B_2$ from molten Al. In that study, fluxing of the molten Al with agitation was recommended. However, Cr removal as Cr-borides was not reported. Removal of Zr, Ti, V, Cr and Mn from molten Al by adding boron-bearing substances on industrial scale has also been developed [30]. However, excess boron addition was the key finding assuming transition metal diborides formation in molten Al. CrB_2 proportion was only 2% while calculating B addition in molten Al. There was no evidence of CrB_2 formation in molten Al or even samples collected from bottom of the crucible. SETZER and BOONE [31] reported the effect of Cr content on electrical conductivity of Al, but no evidence related to CrB_2 was reported. It was quantified that addition of 0.0138 wt.% V, 0.0126 wt.% Cr and 0.0175 wt.% Ti will reduce electrical conductivity of Al by 1.0% IACS (international annealed copper standard). Such a decline in electrical conductivity impedes the utilization of Al for electrical conductor applications. Several researchers in Refs. [13,14,32] proposed reaction mechanisms of transition metal impurities with B-bearing substances. Al−B master alloys (AlB_{12} and AlB_2) were used for removal of Ti, V and Cr in the form of their stable borides. The decay in transition metal impurities was logarithmic, thereby the increase in electrical conductivity was exponential with reaction time. The sludge collected from bottom of the crucible contained 45% Ti, 33% V and >10% Cr, possibly as their borides. Electrical conductivity increased with the increase of reaction time after addition of B-bearing substances, which was key focus of previous researchers. WANG et al [33] investigated the borides sludge and action mechanism of AlB_2 with commercial purity Al (99.7% pure). The sludge was composed of α(Al) matrix, hexagonal particles of undissolved AlB_2, lath-shaped particles of $FeAl_3$ and fine clusters of transition metal borides (Ti, V, Zr and Fe). There is no evidence of Cr-borides formation in the sludge. The findings in Ref. [33] disagreed with those reported in Ref. [29]. KARABAY and UZMAN [1,2] investigated boron treatment process on industrial scale and removal of Ti, V and Cr impurities from smelter grade Al. During the study, the increase in Al electrical conductivity was treated as removal of Ti, V and Cr. Fine TiB_2, VB_2 and CrB_2 particles were not detected during SEM and

subsequent analyses. Only peaks of Si, Ti and B were possible to be detected during EDX analysis.

Despite several great attempts, removal of Cr and formation of stable Cr-borides (CrB_2, CrB, Cr_3B_4 or Cr_5B_3) during boron treatment process are still not understood very well. In addition, there are no sound investigations to find out Cr-borides formation in the presence of V in Al.

This study therefore focused on understanding the mechanism of Cr removal from molten Al by adding Al−4%B (AlB_{12}) master alloys in the presence of V at 1023 K. The structure of this manuscript was designed as follows: Firstly, a thermodynamic analysis of Al−B, Al−Cr, Al−V, Cr−B, V−B was performed and their respective Al−Cr−V−B phase diagrams were developed. These thermodynamic predictions provided a platform for further experimental studies. Then, the mechanisms of Cr and V borides formation were discussed followed by the kinetics of AlB_{12} reaction with Cr and V. Finally, a reaction mechanism was proposed based on experimental findings, and critical analysis was presented based on the findings of present study and those found in Refs. [29,30,33].

3 Thermodynamic analysis

The thermodynamic analysis of Al−B, Al−Cr, Al−V, Cr−B, V−B and Al−Cr−V−B phase diagrams was discussed in this section. Al−B binary phase diagram analysis is important to understand thermodynamically stable phases at room temperature. During boron treatment process, B is added as Al−4%B, Al−5%B, Al−6%B, and Al−10%B master alloys. B has a limited solubility (~0.0001 wt.%) in Al in the solid state. In the liquid state, this solubility is however 8 times greater than that reported in Ref. [34]. Al−B binary phase diagram was investigated earlier in Refs. [35,36]. Al, AlB_2, α-AlB_{12}, β-AlB_{12}, AlB_{10} and β-B are the stable phases, and γ-AlB_{12}, α-B, β-B and B(tetragonal) are the metastable phases in the Al−B binary system. Industrially, AlB_2 and AlB_{12} based A−B master alloys as waffles, rods and wires are manufactured for boron treatment of molten Al. Similar to B, Cr also exhibits limited solubility in the solid Al. Al−Cr binary phase diagram is shown in Fig. 2 [37,38].

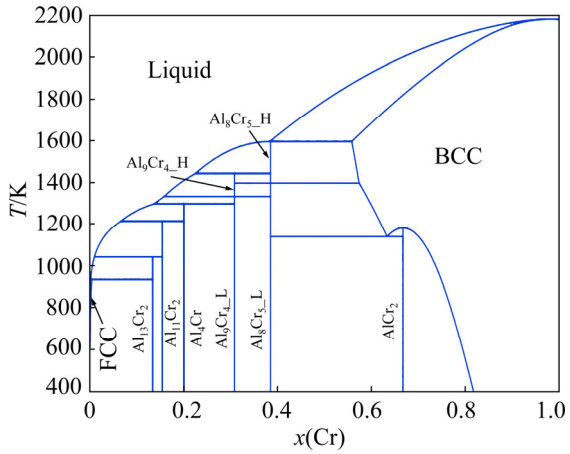

Fig. 2 Al−Cr binary phase diagram [37,38]

Al, $Al_{13}Cr_2$ (Al_7Cr), $Al_{11}Cr_2$(Al_5Cr), Al_4Cr, Al_9Cr_4, Al_8Cr_5, $AlCr_2$ and Cr are the stable phases. In the Al-rich corner of Al−Cr binary phase diagram, Al_7Cr is the only stable phase at room temperature. Al−V binary phase diagram analysis has been reported elsewhere [6]. Al, $Al_{21}V_2$ ($Al_{10}V$), $Al_{45}V_7$ (Al_7V), $Al_{23}V_4$ (Al_6V), Al_3V, Al_8V_5, AlV_3 and V are thermodynamically stable phases at room temperature [39]. CrB, CrB_2, Cr_2B, Cr_4B, Cr_3B_4 and Cr_5B_2 are stable borides in the Cr−B binary system. In the V−B binary system, VB, VB_2, V_3B_4, V_3B_2, V_5B_6 and V_2B_3 are possible boride phases at room temperature. It has been reported that the transition metal diborides (CrB_2, VB_2, TiB_2 and ZrB_2) are more stable phases than their sibling phases [23]. These predictions are based on the Gibbs free energy minimisation from 650 to 900 °C using the HSC chemistry thermodynamic software. Thermodynamic analysis of the Al−0.50%Cr−0.50%V−0.42%B and Al−0.50%Cr−0.50%V−0.73%B systems has been studied earlier [6]. Stoichiometric and 75% excess of stoichiometric B additions were investigated, which were suggested in Ref. [6] for efficient boron treatment process. Figure 3 [6] shows changes in the solutes (V, Cr and B) and stable borides (VB_2 and AlB_2) equilibrium concentrations in molten Al with temperature.

The concept of adding excess B during boron treatment process was tested during thermodynamic analysis. It was predicted that Cr removal by adding stoichiometric or excess B in molten Al is not feasible. There is no evidence of stable CrB_2 formation even in the case of excess B in Al solution. It is predicted that excess B will react with Al to form AlB_2 as shown in Fig. 3(b).

The literature survey [12,29−33] and the thermodynamic analysis revealed that the CrB_2 formation and removal of Cr from molten Al during boron treatment process are disputed and need further investigation. Several researchers [30,31,33] reported the Cr-borides formation during the sludge analysis. In this study, the removal of Cr from molten Al in the presence of V was investigated experimentally. The findings of this study will provide a platform to manage and control Cr impurities in the smelter grade Al.

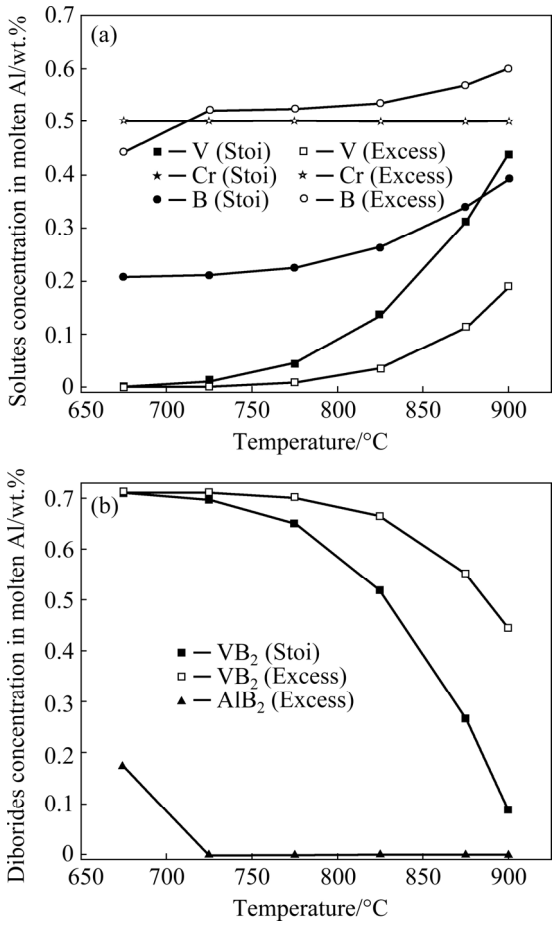

Fig. 3 Solutes (a) and diborides (b) equilibrium concentrations in Al−0.50%Cr−0.50%V−0.42%B and Al−0.50%Cr−0.50%V−0.73%B alloys (Stoi: Stoichiometric B addition; Excess: 75% excess B addition) [6]

4 Experimental

4.1 Materials

Materials used in this study were high purity Al ingots, Al−4%B, Al−20%Cr and Al−10%V master alloys. The master alloys were acquired from KBM AFFILIPS, B.V, Netherlands and KB Alloys, AMG Al, USA. High purity Al (99.90%) ingots were supplied by the Materials Science and Engineering, Commonwealth Scientific and Industrial Research Organisation (CSIRO), Clayton, Victoria, Australia. Chemical compositions of Al ingots and Al master alloys were reported elsewhere [6]. High purity Al contains 0.0027 wt.% V, 0.0032 wt.% Ti, 0.021 wt.% Fe, and 0.0005 wt.% Cr. Figure 4 shows optical microscopy (OM) images of Al−4%B and Al−10%V master alloys. Black particles in Fig. 4(a) are AlB_{12}, which are in clusters. These particles vary from ~1 to >100 μm. Contrary to that, AlB_2 particles exhibit high aspect ratio. AlB_2 particle diameters change from 1 to 5 μm and length from 10 to 200 μm. AlB_2-based alloys are used in launders and continuous casting lines due to shorter reaction time. However, AlB_{12}-based Al−B master alloys are used in the holding furnaces where longer reaction time is allowed. Figure 4(b) shows OM image of Al−10%V master alloy, which is composed of Al matrix reinforced with two distinct intermetallic (IMC) particles. $Al_{10}V$ and Al_7V are stable phases at room temperature. Al_7V is a primary phase which precipitates prior to alloy solidification. However, $Al_{10}V$ precipitates during the later stage of the solidification. Al−20%Cr master alloy is composed of Al_7Cr, Al_5Cr and Al_4Cr intermetallic phases used in this study.

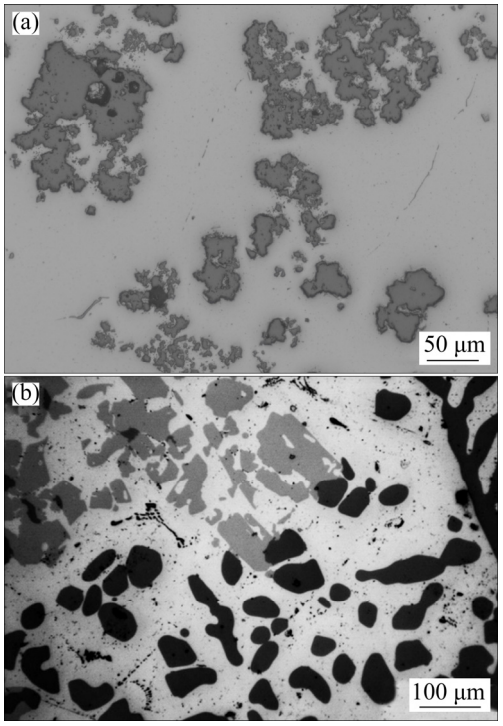

Fig. 4 OM images of Al−4%B (AlB_{12}) (a) and Al−10%V ($Al_{10}V$ and Al_7V) (b) master alloys

4.2 Experimental plan

A weighed amount of pure Al ingot was firstly melted in a boron-nitride (BN) coated clay bonded graphite crucible in a resistance pot furnace as shown in Fig. 5. Subsequently, Al−10%V and Al−20%Cr were added in the molten Al at 1023 K. It was aimed to prepare an Al−0.50%V−0.50%Cr molten alloy containing both V and Cr in solution instead of their $Al_{10}V$, Al_7V, Al_7Cr, Al_5Cr and Al_4Cr intermetallic particles. To achieve homogenous distribution of alloying elements in molten Al, the mixture was held at 1023 K for 24 h and intermittently stirred manually using alumina rod. Temperature was controlled within ±2 K using a K-type thermocouple which was inserted in the molten bath, as depicted in Fig. 5. Weighed Al−4%B(AlB_{12}) ingots were added in the Al−0.50%V−0.50%Cr mixture at 1023 K. Molten alloy samples were taken at 0, 5, 10, 15, 30, 45 and 60 min after adding Al−B master alloy ingots. Samples were solidified in air and preserved for further analysis. Experimental plan used in this study is listed in Table 2. Both CrB_2 and VB_2 phases are assumed to form in the molten Al−0.50%Cr−0.50%V−0.419%B alloy. For this, required amount of B as Al−B (AlB_{12}) master alloy ingots was prepared and added at 1023 K. The melt was stirred manually before taking each sample using steel scoop. If both Cr and V have the same affinity to form their stable borides, they will form in equal proportion by reacting with B. This will result in decline in both Cr and V contents in the Al−0.50%Cr−0.50%V−0.419%B alloy with increasing time.

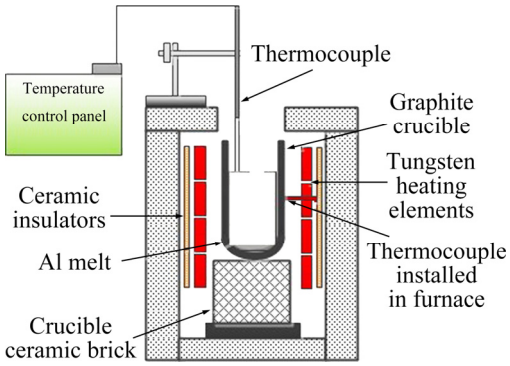

Fig. 5 Schematic diagram of resistance heating pot furnace

Table 2 Experimental plan for preparation of Al−0.50%Cr−0.50%V−0.419%B alloy

Level of B addition	Melting practice	Temperature/ K	Sampling time/ min
0.419%	Resistance pot	1023±2	0, 5, 10, 15, 30, 45, 60

Al−B(AlB_{12}) addition was stoichiometric to Cr and V (assuming CrB_2 and VB_2 formation)

4.3 Characterisation techniques

The alloy samples were analyzed for Al−B(B/AlB_{12})/Cr/V reaction product and borides formation. For microstructural features, polished samples were studied under an optical microscope (Leica DM2500) and a scanning electron microscope (FEI NOVA, SEM), equipped with energy dispersive X-ray spectroscopy (EDS). Sample metallography procedure was reported elsewhere [6]. Changes in Cr and V contents of the Al−0.50%Cr−0.50%V−0.419%B alloy were determined using inductively coupled plasma atomic emission spectroscopy (ICP-AES). For ICP-AES analysis, boron-treated Al alloy chips were produced by drilling 5 holes of ~3 mm diameter at different locations of disc samples of 30 mm diameter to ensure a representative sample. The alloy chips (1−2 g) were dissolved in 50% HCl solution that dissolved Al, Cr and V in solution, leaving borides particles in the solid residue. The solution was separated from undissolved borides particles (CrB_2, VB_2, AlB_2/AlB_{12}) and analyzed for Cr and V contents. HNO_3 addition in HCl solution will escalate Al alloy dissolution. However, small amount of borides (CrB_2, VB_2, AlB_2/AlB_{12}) may also dissolve, which hence were not adopted in this study.

5 Results and discussion

In this section, the interaction of Cr and V with [B]/AlB_{12} in molten Al was discussed. The change in reaction product microstructure with reaction time was observed under OM and SEM. Figure 6 shows OM images of Al−0.50%Cr−0.50%V−0.419%B alloy melted and held at 1023 K. The alloy microstructure is composed of IMC particles, Cr/V/B/AlB_{12} reaction product, un-reacted AlB_{12}, and Al matrix. IMC particles are composed of Al, Cr and V ternary or binary elements. At this stage, it is not clear whether these IMCs are binary (Al−V, Al−Cr, V−Cr) or ternary (Al−Cr−V) compounds. Reaction product is the key feature of Fig. 6, which suggests reaction between impurity elements (Cr/V)

and B-bearing substance (AlB_{12}). It is suggested that the AlB_{12} clusters in Al−B master alloy may determine reaction product ring size. The reaction product ring size varies from 50 to more than 200 μm. However, IMC particle size varies from 10 to less than 50 μm. The reaction product ring thickness increases with increasing reaction time, as shown in Fig. 6(b). AlB_{12} presence inside ring suggests that reaction between Cr/V and AlB_{12} is incomplete and the alloy system is far from equilibrium.

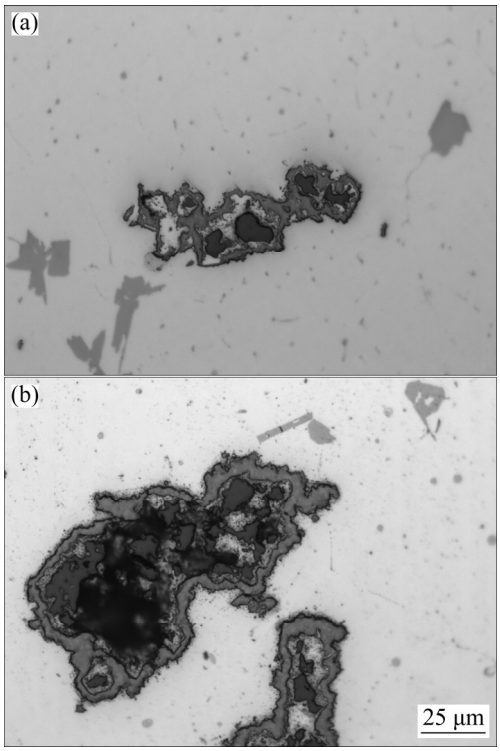

Fig. 6 OM images of Al−0.50%Cr−0.50%V−0.419%B alloy melted and held at 1023 K and different time: (a) 15 min; (b) 60 min

Theoretically possible reactions during the boron treatment of Al−0.50%Cr−0.50%V alloy with [B]/AlB_{12} can be written as follows:

$$AlB_{12(s)}=[Al]+12[B] \quad (1)$$

$$[Cr]+2[B]=CrB_{2(s)} \quad (2)$$

$$Al_7Cr_{(s)}+2[B]=CrB_{2(s)}+7[Al] \quad (3)$$

$$Al_5Cr_{(s)}+2[B]=CrB_{2(s)}+5[Al] \quad (4)$$

$$Al_4Cr_{(s)}+2[B]=CrB_{2(s)}+4[Al] \quad (5)$$

$$6[Cr]+AlB_{12(s)}=6CrB_{2(s)}+[Al] \quad (6)$$

$$[V]+2[B]=VB_{2(s)} \quad (7)$$

$$Al_{10}V_{(s)}+2[B]=VB_{2(s)}+10[Al] \quad (8)$$

$$Al_7V_{(s)}+2[B]=VB_{2(s)}+7[Al] \quad (9)$$

$$6[V]+AlB_{12(s)}=6VB_{2(s)}+[Al] \quad (10)$$

Here the notion [ ] represents the element is in solution with molten Al, and (s) is used to represent the solid phases. Initially, [B] in solution with Al will react with [Cr]/[V] to form their stable borides depending on their relative reaction potential in molten Al. Reactions (2) and (7) are favourable compared to other reactions. Thermodynamically, direct chemical reaction of [B] with [Cr]/[V] is favourable compared to first dissolution of the solid phases (Al_7Cr, Al_5Cr, Al_4Cr, $Al_{10}V$, Al_7V) (Reactions (3)−(6) and (8)−(10)) followed by their chemical reaction. The reacting element [B] availability is related to the solid AlB_{12} particles dissolution (Reaction (1)) in molten Al, which is the slowest process. Industrially, Al boron treatment time is determined by the AlB_2 and AlB_{12} particle sizes. This is directly related to the available surface area for chemical reaction, hence borides formation in molten Al.

The SEM images of the samples taken after 0, 5, 15, 30, 45 and 60 min are shown in Fig. 7. The sample taken at 0 min shows undissolved Al, V, Cr IMC particles in the Al matrix, Fig. 7(a). It is suggested that these IMC particles precipitate during solidification process as solubility of both Cr and V is limited in Al at room temperature. One of the key features of the Cr and V reaction with AlB_{12} is the reaction product ring formation as shown in Fig. 7. The reaction product ring is composed of (Cr,V) borides, surrounding the undissolved AlB_{12} particles. Such characteristic boride rings have been reported in Refs. [26,29] while investigating Zr and V removal from molten Al. AlFeSi IMC is also formed in the Al alloy, as shown in Fig. 7(c). Similarly, COOPER and KEARNS [13] reported transition metal impurities removal as borides which form rings during reaction with Al−AlB_{12} master alloys. A common feature of boride ring formation agrees with the previous studies [13,23]. It is, however, not clear whether these borides rings are composed of the Cr, V or a solid solution of both $(Cr,V)B_2$ borides.

EDS analysis results of sample taken after 45 min of reaction are shown in Fig. 8. The sum spectrum in Fig. 8(b) confirms Al, Cr, V and B in the alloy. The V and Cr contents detected are higher than the initially added contents. This is linked to

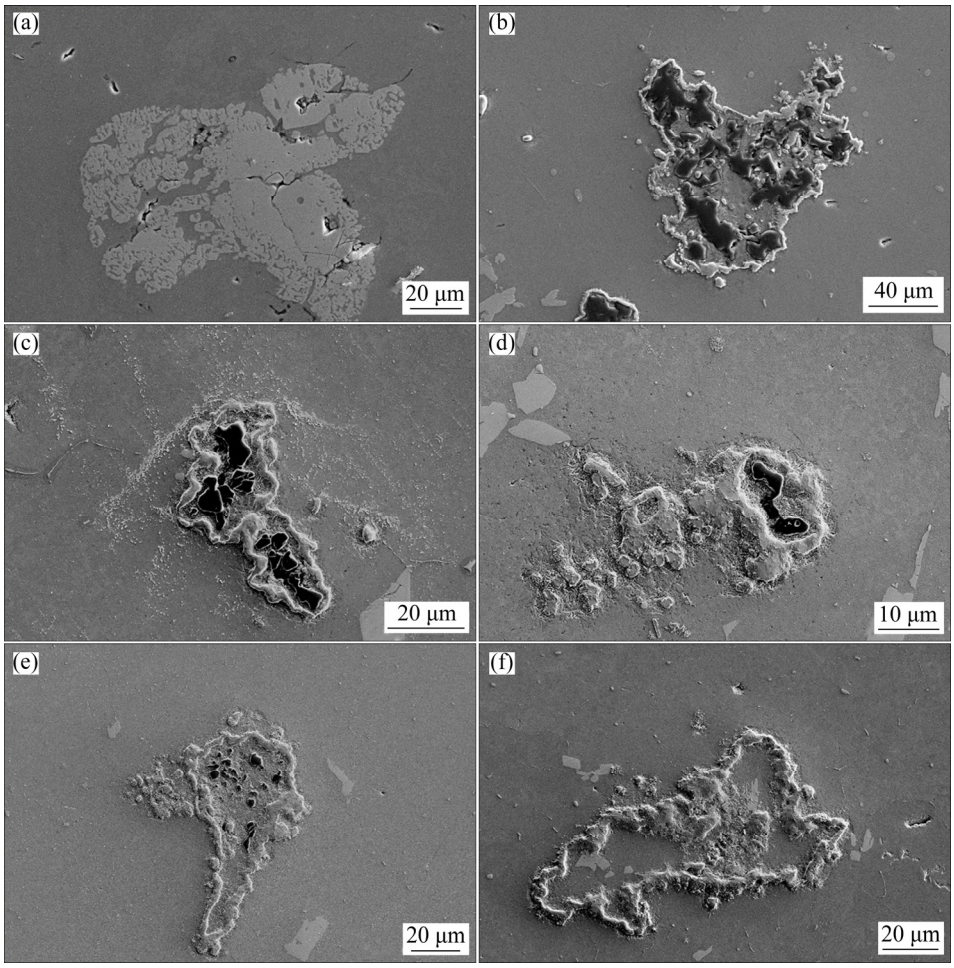

Fig. 7 SEM images of Al−0.50%Cr−0.50%V−0.419%B alloy melted and held at 1023 K and different time: (a) 0 min; (b) 5 min; (c) 15 min; (d) 30 min; (e) 45 min; (f) 60 min

the reaction with B/AlB_{12} and Al, Cr, V IMC formation during the solidification of molten samples in the selected region. Undissolved black phase inside the reaction product ring (Point 1) is composed of Al and B which represent AlB_{12} particles/clusters as given in Fig. 8(c). The EDS analysis of the reaction product ring reveals a solid solution of Al, Cr and V borides, Point 2 in Fig. 8(a). The boride ring EDS analysis suggests the formation of Cr and V borides by reacting with [B]/AlB_{12}. The Cr borides formation in molten Al in the presence of V is not well understood. Al and Cr are likely to be detected from the base Al matrix during EDS analysis. A quantitative analysis is reliable to establish Cr-borides formation in molten Al−Cr−V−B alloy at 1023 K. The EDS analysis results of Al, V and Cr IMCs are shown in Fig. 8(e). It indicates a ternary Al−Cr−V IMC formation rather than binary $Al_{10}V$ or Al_7Cr, as reported during thermodynamic analysis in the earlier section.

Microscopy and EDS analyses revealed that the following conclusions.

(1) Initially, the reactions between [Cr] and [V] with [B]/AlB_{12} were fast. This was observed during the formation of product ring within the first 5 min of reaction. Later, the reaction rate declined due to solid Cr/V boride rings growth which restricted reactants (B, V and Cr) mass transfer. The boride ring formation feature is in an agreement with the previous studies. A marginal increase in boride ring thickness with time suggests that the later reaction stage is controlled by mass transfer through the solid phase rather than the liquid phase.

(2) Undissolved AlB_{12} particles encapsulated by the boride ring advocate that the overall reaction is incomplete. Ideally, AlB_{12} should dissolve, release [B] and be consumed with time to form Cr/V borides. It is noted that the Al−0.50%Cr−0.50%V−0.419%B alloy is far from equilibrium. Practical measures including Al bath stirring should be taken to enhance the AlB_{12} dissolution rate for

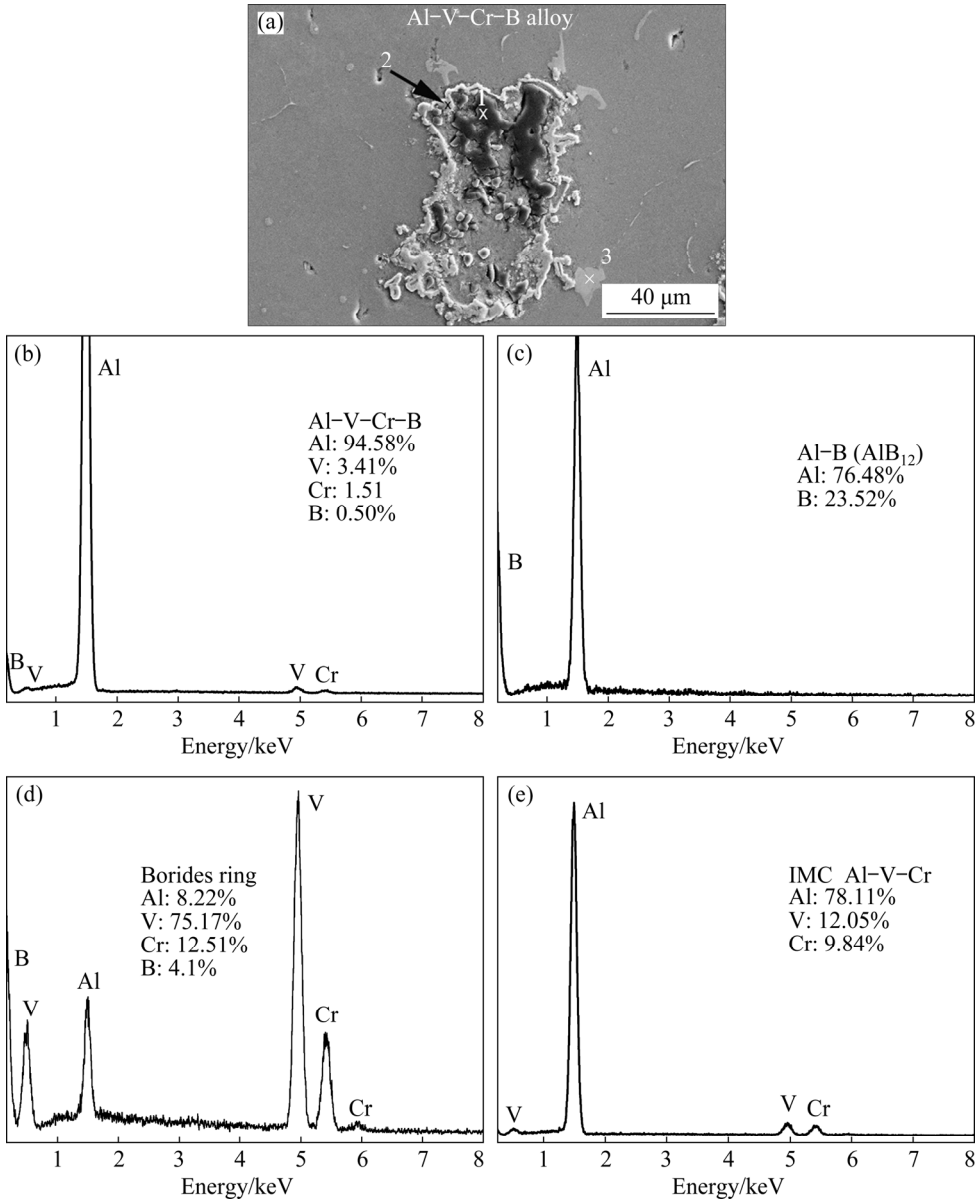

Fig. 8 SEM image (a) and EDS analysis spectra (b−e) of Al−0.50%Cr−0.50%V−0.419%B alloy sample collected after reaction for 45 min: (b) Sum spectrum; (c) Undissolved Al−B particles; (d) Reaction product/boride ring; (e) Al−Cr−V IMC particles

efficient boron treatment process.

(3) Cr evidence in the boride ring is not conclusive as results are based on the qualitative EDS analysis. A quantitative analysis will confirm Cr-borides formation in molten Al by adding Al−B master alloy.

Predominantly, the boride ring morphology in the Al−Cr−V−B alloys is similar to the Al−V−B alloy as reported earlier [6]. This points out that reaction mechanism of [B]/AlB_{12} might be similar to that of the Al−V−B alloy [6,23]. However, boride rings observed in this study are denser than those of the Al−0.50%Zr−0.50%V−0.115%B alloy [29].

6 Kinetics of Cr and V removal from molten Al

The kinetics of Cr and V removal from molten Al was investigated in this section. For laboratory experiments, it is hypothesized that both Cr and V will react simultaneously with [B]/AlB_{12} to form their stable borides (CrB_2 and VB_2) at 1023 K. As a result, the decline in Cr and V contents in molten Al−0.50%Cr−0.50%V−0.419%B alloy will follow similar trends. Samples collected at regular intervals were analyzed for Cr and V in solution

with molten Al by ICP-AES and their change with reaction time is shown in Fig. 9. Both Cr and V exhibit entirely different reaction mechanisms with [B]/AlB_{12}. Cr contents (0.50%) are unchanged during reaction time studied (60 min). An increase in Cr concentration is attributed to dissolution of solid Al−Cr (Al_7Cr, Al_5Cr, Al_4Cr) IMC particles. Overall, there is no change in Cr concentrations after adding Al−B master alloy, which indicates the fact that [Cr] does not react with [B]/AlB_{12} to form their borides.

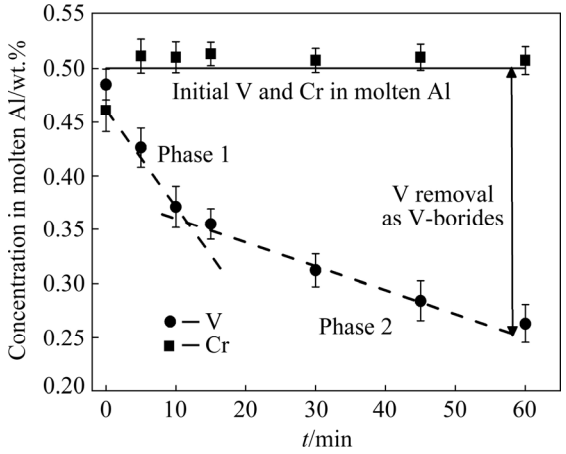

Fig. 9 Changes in Cr and V concentrations with reaction time in Al−0.50%Cr−0.50%V−0.419%B alloy melted at 1023 K

It is worth noting that the current findings contradict with the results reported in Refs. [1,2,13,14,26,27]. However, these are in agreement with thermodynamic predictions reported in Ref. [27]. The kinetics of V removal demonstrates two distinct reaction rates in molten Al, as shown in Fig. 9. Phase 1 and Phase 2 respectively represent early stage (0−10 min) and later stage (10−60 min) of reactions between V and [B]/AlB_{12}. During Phase 1, V concentration drops from 0.485 wt.% to 0.371 wt.%. Phase 2 represents slower reaction rate, thereby, V concentration decreases from 0.371 wt.% to 0.263 wt.%. It is observed that reaction rate is faster initially when Al−B master alloy is added to the Al melt containing Cr and V in solution. Factors such as [B] in solution and un-reacted surface area of AlB_{12} facilitate higher reaction rate during Phase 1. [B] and un-reacted AlB_{12} will deplete with time in the Al melt. The boride rings that encapsulate the black AlB_{12} particles will provide barrier to [Cr]/[V] mass transfer to reach AlB_{12} particles. As a result, it is expected that reaction rate will slow down with increasing time.

In addition, AlB_{12} dissolution and [B] mass transfer across the boride ring will be obstructed because of diffusion barrier that increases with the increase of reaction time. Therefore, Phase 2 exhibits much slower reaction rate than Phase 1. It is observed that two distinct reaction mechanisms operate during V/Cr reactions with B/AlB_{12}. Therefore, these were investigated separately. It is postulated that Phase 1 reaction is controlled by [V] and [B] mass transfer in the liquid Al−0.50%Cr−0.50%V−0.419%B alloy. However, Phase 2 reaction is controlled by [V] and [B] mass transfer through the solid phase (boride ring). These hypotheses will be critically analyzed against established models in Refs. [20,36,39].

The kinetics of V removal from the smelter grade Al during industrial boron treatment trials has been reported earlier [25]. Overall, V reaction kinetic was faster in early stage of reaction which slowed down with increasing time. It is advocated from industrial trials that Cr exhibits different kinetics compared to V. Moreover, there is no evidence that CrB_2 is formed from Cr in the smelter grade Al.

The Cr and V removal from molten Al−0.50%Cr−0.50%V−0.419%B alloy in the form of their borides (CrB_2 and VB_2) is plotted using the conversion (α) approach which is widely used during chemical reaction studies. Initially, Cr conversion is higher due to incomplete Al−Cr IMC dissolution during melting process. As a result, 0.039% Cr was tied as IMC (Al_7Cr and Al_5Cr) in molten Al, which was dissolved with time raising. There is no evidence of Cr removal from molten Al−0.50%Cr−0.50%V−0.419%B alloy, as shown in Fig. 10. Contrary to that, more than 45% V is removed from molten Al alloy in the form of their borides. During Phase 1, 50% of the total V was converted into VB_2 borides. The remaining 50% was removed in 50 min (Phase 2). It is noted that the reaction rate during Phase 1 is approximately 5 times faster than that during Phase 2.

6.1 Phase 1: Mass transfer through liquid phase control

It is hypothesised that VB_2 formation is first order with respect to V concentration and reaction rate is controlled by [V] and [B] mass transfer

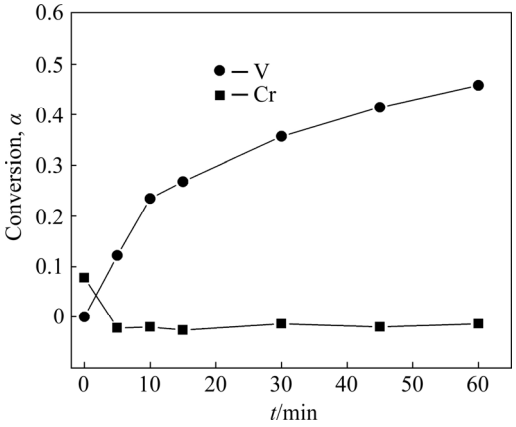

Fig. 10 Conversions of Cr and V from Al−0.50%Cr−0.50%V−0.419%B alloy at 1023 K

during Phase 1 (0−10 min) in molten Al−0.50%Cr−0.50%V−0.419%B alloy at 1023 K. Hence, Phase 1 experimental data are plotted against the mass transfer through liquid phase-controlled model [24,40], as shown in Fig. 11. The integrated rate relationship for the liquid phase mass transfer controlled chemical reactions is given in Eqs. (11) and (12):

$$Y\ln Z=-kt \tag{11}$$

$$Y=\left(\frac{V_m}{A}\right)\frac{(c_0-c_e)}{c_0},\quad Z=\frac{c-c_e}{c_0-c_e} \tag{12}$$

where V_m, A and k are the volume, interfacial area (AlB_{12} and V) and reactants mass transfer coefficient through the liquid Al−0.50%Cr−0.50%V−0.419%B alloy, respectively; t is the reaction time; c_0, c_e and c are concentrations of V at time t=0, equilibrium at 1023 K, and at time t, respectively. Interfacial area of reacting species (AlB_{12} in this case), which is continuously changed with reaction time, is not constant. For convenience, Al alloy volume (V_m) and interfacial area (V and AlB_{12}) are assumed to be constant. The AlB_{12} interfacial area was calculated by counting their clusters/particles in the Al−4%B master alloy as reported in Ref. [6]. For kinetics study, similar approaches have been adopted by the previous investigators [24,29]. The Phase 1 experimental data are plotted using integrated rate law (Eq. (11)), see Fig. 11. The best fit between experimental data and liquid phase mass transfer-controlled model confirmed that Phase 1 reaction is controlled by the mass transfer of [B] and [V] through the liquid phase. The confidence level of these findings is 99% (i.e., R^2=0.99), as reported in Fig. 11. In addition, mass transfer coefficient (k_m) is 9.6×10^{-4} m/s, which is also within the range (10^{-3} to 10^{-4} m/s) reported for a typical solid−liquid reactions [41]. The mass transfer coefficient of [V] (k_m=9.6×10^{-4} m/s) is similar to that reported earlier [24]. However, these k_m values are about 1% as high as that of [Zr] (k_m=1.65×10^{-2} m/s) as reported in Ref. [29]. A summary of the mass transfer coefficients of selected alloy systems under various processing conditions is given in Table 3.

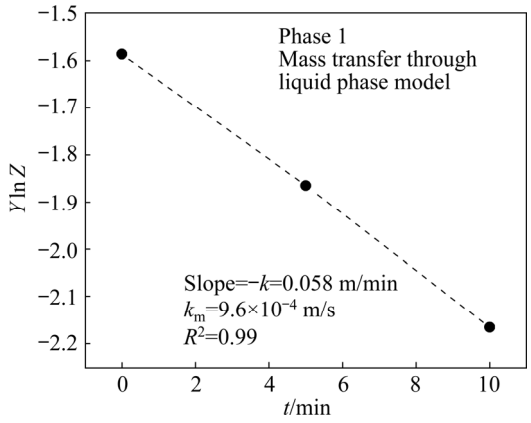

Fig. 11 Integrated rate plot for V removal from molten Al−0.50%Cr−0.50%V−0.419%B alloy at 1023 K from 0 to 10 min of reaction (Phase 1)

6.2 Phase 2: Mass transfer through solid layer control

It is assumed that the Phase 2 reaction kinetics is controlled by the mass transfer/diffusion of reacting species [B]/[V] through the boride ring (VB_2). Solid−liquid diffusion models have been developed earlier [42−44]. Solid AlB_{12} particles dissolution and [V] diffusion through boride ring are the key steps. Ginstling−Brounshtein (GB) [43] and Jander [42] models (Eqs. (13) and (14)) depict shrinking of the solid core and formation of products ring similar to that observed in this study.

$$1-(2/3)\alpha-(1-\alpha)=k't \tag{13}$$

$$[1-(1-\alpha)]^{2/3}=k't \tag{14}$$

where α is V conversion from solution into VB_2 with reaction time t after the addition of Al−B (AlB_{12}) master alloys into Al−0.50%Cr−0.50%V−0.419%B alloy melt; k' is the reaction rate constant that depends on concentration gradients of reacting species [B] and [V], molar density of the solid product layer (VB_2), and diffusion coefficients of the reacting species [B] and [V]. An interfacial

Table 3 Summary of Cr, V and Zr mass transfer coefficients (k_m) in molten Al

Experiment	Impurity concentration	Stirring time/min	Stirring energy/(W·t^{-1})	K_m/(m·s^{-1})	Source
Laboratory	Cr: 0.50%, V: 0.50%	14 (Natural+manual)	9.72×10^{-6}*	9.6×10^{-4}	This study
Laboratory	Zr: 1.00%	60 (Induction)	9.32×10^{-2}	9.5×10^{-4}	[28]
Plant trial 1#	V: 0.0068%	2 (Light mechanical)	10^{-4}–10^{-5}**	1.08×10^{-4}	[25]
Plant trial 1#	V: 0.0080%	2 (Light mechanical)	10^{-4}–10^{-5}**	1.32×10^{-4}	[25]
Laboratory	V: 0.0350%	60 (Induction)	9.32×10^{-2}	2.25×10^{-2}	[24]
Laboratory	V: 0.0350%	60 (Induction+Ar)	9.63×10^{-2}	2.00×10^{-1}	[24]
Laboratory	V: 1%	60 (Natural convection)	9.72×10^{-6}*	2.15×10^{-3}	[6]
Laboratory	V: 1%	60 (Induction)	9.32×10^{-2}	6.2×10^{-4}	[24]
Laboratory	V: 1%	10 (Ar)	3.06×10^{-3}	5.8×10^{-3}	[24]

*Estimated values of stirring energy by comparing natural and manual stirring mechanisms; **Stirring energy calculated using estimated melt velocity

area between the solid core and the reaction product is assumed to be constant in the Jander diffusion model, hence underestimating the reaction kinetics. Therefore, the experimental data reported in this study were not plotted using the Jander model [42]. The GB diffusion model [43] is a better choice for reaction rate constant prediction in this study. The left-hand side of Eq. (13) is plotted against the reaction time t as shown in Fig. 12, which shows the curve fitting value (R^2) of the Phase 2 experimental data of 0.98 and a reaction rate constant k' of 1.02×10^{-6} s^{-1}. A rate constant of 3.42×10^{-6} s^{-1} was reported for spinel ferrite formation in the diffusion through solid layer solid−liquid system. For ZrB_2 formation in Al−Zr−B system, a rate constant value of 1.12×10^{-5} s^{-1} was reported. The rate constant values obtained in this study are in agreement with the values reported earlier [45]. A disagreement in rate constant values compared to Al−Zr−B alloy [28] are related to less

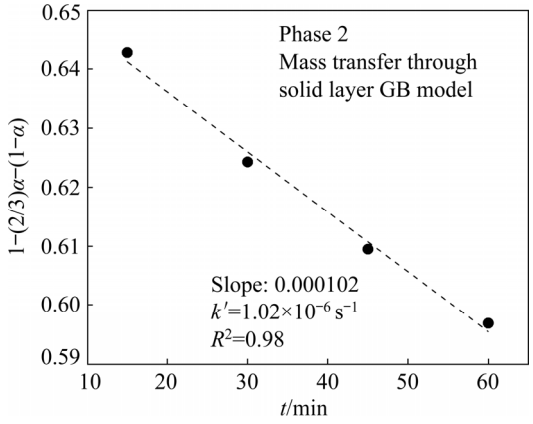

Fig. 12 Phase 2 (10−60 min) experimental data plotted against reaction time by using Ginstling−Brounshtein (GB) diffusion model

thickness of the boride ring and melting in induction furnace (higher melt stirring). It was observed that the Phase 2 reaction kinetic is controlled by the mass transfer/diffusion of the reacting species [B] and [V] through the boride ring (VB_2). It also implied that the Phase 2 reaction might be accelerated by interrupting the boride ring formation which can be achieved by melt stirring with inert gas.

7 Mechanisms of Cr and V removal from molten Al

Based on the thermodynamic, microstructural and kinetics analyses, a mechanism of Cr and V removal from molten Al−0.50%Cr−0.50%V−0.419%B alloy is proposed. The boron treatment process is divided into six steps as shown in Fig. 13. Al−B master alloy ingots composed of AlB_{12} particles/clusters are added into the Al alloy. It is assumed that Cr and V are in solution with molten Al alloy at 1023 K, as depicted in Step 1. A chilled layer of molten Al develops around Al−B master alloys and eventually dissolves within few seconds, releasing [B] and AlB_{12} particles/clusters into the molten Al alloy (Step 2). At this stage, B in solution reacts immediately with [V] and forms stable VB_2 particles. Simultaneously, [V] from molten Al alloy transfers to AlB_{12} followed by a chemical reaction and forms VB_2 particles (Step 3). These steps are completed within the first 10 min of reaction and demonstrate faster reaction rates which are controlled by mass transfer of both [B] and [V] in the molten Al alloy, as shown in Fig. 11. A solid−liquid reaction takes over the later stages of the reaction, see Steps 4−6. Solid AlB_{12} particles are

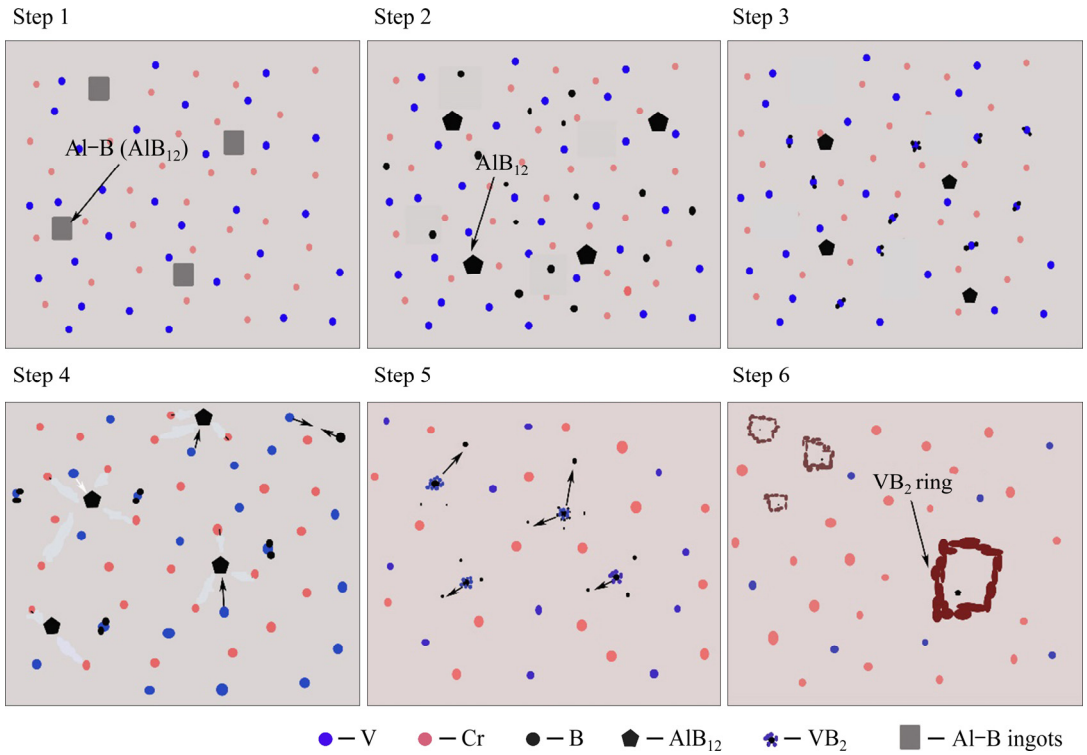

Fig. 13 Schematic diagrams of V and Cr interacting with AlB_{12} master alloy

dissolved and reaction product ring (VB_2) becomes thick with reaction time. As a result, the reaction rate of VB_2 formation slows down gradually as designated by the Phase 2. It was noted that the Cr removal from molten Al−0.50%Cr−0.50%V−0.419%B alloy is not feasible by adding AlB_{12}. The excess [B] in the alloy forms AlB_2 particles rather than CrB_2. Figure 13 shows only removal of [V] and formation of VB_2 particles/rings. Cr atoms will remain in solution and will react with Al to form Al−Cr IMC particles (Al_7Cr, Al_5Cr and Al_4Cr) during the solidification process.

For efficient boron treatment process, it is recommended to interrupt the boride rings formation through intermittent stirring of the Al alloy melt. The chemical reactions (Reactions (1) to (10)) can be accelerated by [B] and [V] mass transfer and the boride rings (VB_2) breakage. This would accelerate solid phase (AlB_{12}) dissolution, thereby providing fresh [B] for chemical reaction with [V] to form VB_2. A multistage addition of the Al−B master alloys can promote efficiency of the industrial boron treatment process.

8 Conclusions

(1) CrB_2 is the most stable phase compared to other possible Cr-boride phases (CrB, Cr_2B, Cr_4B, Cr_3B_4 and Cr_5B_2) at 1023 K as predicted by the thermodynamic analysis.

(2) Cr removal from molten Al in presence of other transition metals (V, Ti, Zr) in the form of CrB_2 is not feasible. Excess [B] in molten Al will form AlB_2 and VB_2 rather than CrB_2 particles during boron treatment process.

(3) The early-stage reaction is faster between [V] and [B]/AlB_{12} and is controlled by the mass transfer of [B]/[V] through the liquid phase. The calculated mass transfer coefficient (k_m) is 9.6×10^{-4} m/s, which is within the range of (10^{-3}−10^{-4}) m/s for the similar solid−liquid reactions.

(4) The later stage reaction (10−60 min) is controlled by diffusion through the solid boride ring (VB_2). Experimental data plotted against the Ginstling−Brounshtein (GB) diffusion model confirmed the hypothesis. The rate constant for this phase is 1.02×10^{-6} s^{-1}, which is within the range (1.67×10^{-6} s^{-1}) for similar systems.

(5) Overall, kinetics of V removal from molten Al in the presence of Cr is in agreement with the earlier work. The current study findings support the argument that Cr does not play a significant role by reacting with [B]/AlB_{12} during boron treatment process.

(6) Finally, a reaction mechanism of boron

treatment process of molten Al for the removal of Cr and V is proposed in this study. It is identified that Cr does not affect the kinetics of V removal from molten Al.

Acknowledgments

This work was financially supported by Taif University Researchers Supporting Project (No. TURSP-2020/293), Taif University, Taif, Saudi Arabia. Authors acknowledge RMMF microscopy facility, RMIT University, Australia, for Al alloy samples characterization.

References

[1] KARABAY S, UZMAN I. Inoculation of transition elements by addition of AlB_2 and AlB_{12} to decrease detrimental effect on the conductivity of 99.6% aluminium in CCL for manufacturing of conductor [J]. Journal of Materials Processing Technology, 2005, 160(2): 174−182.

[2] KARABAY S, UZMAN I. A study on the possible usage of continuously cast aluminium 99.6% containing high Ti, V, and Cr impurities as feedstock for the manufacturing of electrical conductors [J]. Materials and Manufacturing Processes, 2005, 20(2): 231−243.

[3] DEAN W A. Effects of alloying elements and impurities on properties [J]. Aluminum, 1967, 1: 174.

[4] GAUTHIER G G. The conductivity of super-purity aluminium: The influence of small metallic additions [J]. Journal of the Institute of Metals, 1936, 59: 129−150.

[5] GRJOTHEIM C K, MALINOVSKY M, MATIASOVSKY K, THONSTAD J. Aluminium electrolysis: Fundamentals of the hall Heroult process [M]. 2nd ed. Dusseldorf: Verlag GmbH, 2004.

[6] KHALIQ A. Thermodynamics and kinetics of transition metal borides formation in molten aluminium [D]. Melbourne: Swinburne University of Technology, 2013: 1−280.

[7] DEWAN M A, RHAMDHANI M A, MITCHELL J B, DAVIDSON C J, BROOKS G A, EASTON M, GRANDFIELD J F. Control and removal of impurities from Al melts: A review [J]. Materials Science Forum, 2011, 693:149−160.

[8] LINDSAY S J. Raw material impurities and the challenge ahead [C]//Proc. Light Metals. TMS, USA, 2013.

[9] ZHANG L, GAO J, DAMOAH L N W, ROBERTSON D G. Removal of impurity elements from molten aluminum: A review [J]. Mineral Processing and Extractive Metallurgy Review, 2011, 32(3): 150−228.

[10] GRANDFIELD J F, KHALIQ A, RHAMDHANI M A, DEWAN M, EASTON M, SWEET L, DAVIDSON C, MITCHELL J, BROOKS G. Melt quality and management of raw material impurities in casthouse [C]//Proceedings of the 10th Australasian Aluminium Smelting Technology Conference. Tasmania, Australia, 2011.

[11] BELL S, DAVIS B D, JAVAID A, ESSADIQI E. Final report on refining technologies of aluminium [R]. Ontario, Canada, 2003.

[12] DUBE G. Removal of impurities from molten aluminium [P]. European patent: A, 1983.

[13] COOPER P S, KEARNS M A. Removal of transition metal impurities in aluminium melts by boron additives [J]. Materials Science Forum, 1996, 217−222: 141−146.

[14] COOPER P S, COOK R, KEARNS M A. Effects of residual transition metal impurities on electrical conductivity and grain refinement of EC grade Al [C]// London: London and Scandinavian Metallurgical Co., Limited, 1997.

[15] CUI X L, WU Y Y, CUI H W, ZHANG G J, ZHAU B, LIU X F. The improvement of boron treatment efficiency and electrical conductivity of AA1070Al achieved by trace Ti assistant [J]. Journal of Alloys and Compounds, 2018, 735: 62−67.

[16] KHALIQ A, RHAMDHANI M A, BROOKS G, GRANDFIELD J A. Analysis of boron treatment using AlB_2 and AlB_{12} based master alloys [C]//Proceedings of the TMS Light Metals. San Diego: Springer, 2014.

[17] ALY I H, OMRAN A M, SHAHEEN M A, BASTAWEESY A. Production of Al−B master alloys from boron-bearing salts using different techniques [C]//Proceedings of the TMS Light Metals. Warrendale: Springer, 2004: 837−841.

[18] WANG X. The formation of AlB_2 in an Al−B master alloy [J]. Journal of Alloys and Compounds, 2005, 403(1−2): 283−287.

[19] GHADIMI H, NEDJHAD S H, EGHBALI B. Enhanced grain refinement of cast aluminum alloy by thermal and mechanical treatment of Al−5Ti−B master alloy [J]. Transactions of Nonferrous Metals Society of China, 2013, 23(6): 1563−1569.

[20] LI J G, HUANG M, MA M, YE W, LIU D, SONG D, BAI B, FANG H. Performance comparison of AlTiC and AlTiB master alloys in grain refinement of commercial and high purity aluminum [J]. Transactions of Nonferrous Metals Society of China, 2006, 16(2): 242−253.

[21] CAI S Q, LI Y J, CHEN Y, LI X W, XUE L H. Effect of nano TiN/Ti refiner on as-cast and hot-working microstructure of commercial purity aluminum [J]. Transactions of Nonferrous Metals Society of China, 2013, 23(7): 1890−1897.

[22] SHARMA R, SINGH A K, ARORA A, PATI S, DE P S. Effect of friction stir processing on corrosion of Al−TiB_2 based composite in 3.5 wt.% sodium chloride solution [J]. Transactions of Nonferrous Metals Society of China, 2019, 29(7): 1383−1392.

[23] KHALIQ A, RHAMDHANI M A, BROOKS G, GRANDFIELD J A. Removal of vanadium from molten aluminum — Part I. Analysis of VB_2 formation [J]. Metallurgical and Materials Transactions B: Process Metallurgy and Materials Processing Science, 2014, 45(2): 752−768.

[24] KHALIQ A, RHAMDHANI M A, BROOKS G, GRANDFIELD J A. Removal of vanadium from molten aluminum—Part II. Kinetic analysis and mechanism of VB_2 formation [J]. Metallurgical and Materials Transactions B: Process Metallurgy and Materials Processing Science, 2014, 45(2): 769−783.

[25] KHALIQ A, RHAMDHANI M A, BROOKS G, GRANDFIELD J A. Removal of vanadium from molten aluminum—Part III. Analysis of industrial boron treatment practice [J]. Metallurgical and Materials Transactions B: Process Metallurgy and Materials Processing Science, 2014, 45(2): 784−794.

[26] KHALIQ A, RHAMDHANI M A, BROOKS G, GRANDFIELD J A, MITCHELL J, CAMERON D. Analysis of transition metal (V,Zr) borides formation in aluminium melt [C]//Proceedings of the European Metallurgical

Conference (EMC). Dusseldorf, Germany, 2011: 825−833.
[27] KHALIQ A, RHAMDHANI M A, BROOKS G, GRANDFIELD J A. Thermodynamic analysis of Ti, Zr, V and Cr impurities in aluminum melt [C]//Proceedings of the TMS Light Metals. San Deigo, USA, 2011: 751−756.
[28] KHALIQ A, RHAMDHANI M A, BROOKS G, GRANDFIELD J A. Thermodynamics and kinetics analyses of ZrB_2 formation in molten aluminium alloys [J]. Canadian Metallurgical Quarterly, 2016, 55(2): 161−172.
[29] KHALIQ A, RHAMDHANI M A, BROOKS G, GRANDFIELD J A. Mechanism of ZrB_2 formation in molten Al−V−Zr alloy during boron treatment [J]. Metallurgical and Materials Transactions B, 2016, 47(1): 595−607.
[30] STILLER W, INGENLATH T. Industrial boron treatment of aluminium conductor alloys and its influence on grain refinement and electrical conductivity [J]. Aluminium (English Edition), 1984, 60(9): 834−837.
[31] SETZER W C, BOONE G W. Use of aluminum/boron master alloys to improve electrical conductivity [C]//Proceedings of the Light Metals. San Diego: Springer, 1992: 837−844.
[32] COOK R, KEARNS M A, COOPER P S. Effects of residual transition metal impurities of electrical conductivity and grain refinement of EC grade aluminum [C]//Proceedings of the Light Metals. San Diego: Springer, 1997: 809−814.
[33] WANG G Q, LIU S H, LI C M, GAO Q. Reaction of boron to transition metal impurities and its effect on conductivity of aluminum [J]. Transactions of Nonferrous Metals Society of China, 2002, 12(6): 1112−1116.
[34] SIGWORTH G K. Grain refining of aluminum and phase relationships in the Al−Ti−B system [J]. Metallurgical Transactions A: Physical Metallurgy and Materials Science, 1984, 15(2): 277−282.
[35] CARLSON O N. The Al−B (aluminum−boron) system [J]. Bulletin of Alloy Phase Diagrams, 1990, 11(6): 560−566.
[36] DUSCHANEK H, ROGL P. The Al−B (aluminum−boron) system [J]. Journal of Phase Equilibria, 1994, 15(5): 543−552.
[37] AUDIER M, DURAND-CHARRE M, LACLAU E, KLEIN H. Phase equilibria in the Al−Cr system [J]. Journal of Alloys and Compounds, 1995, 220(1): 225−230.
[38] CHEN S L, DANIEL S, ZHANG F, CHANG Y A, YAN X Y, XIE F Y, SCHMID-FETZER R, OATES W A. The PANDAT software package and its applications [J]. Calphad, 2002, 26(2): 175−188.
[39] OKAMOTO H. Al−V (aluminum−vanadium) [J]. Journal of Phase Equilibria, 2001, 22(1): 86.
[40] RHAMDHANI M A. Reaction kinetics and dynamic interfacial phenomena in liquid metal−slag systems [D]. Ontario: McMaster University, 2005: 216.
[41] ENGH T A. Principles of metal refining [M]. Oxford: Oxford University Press, 1992.
[42] JANDER W. Realtionen im festen zustande bei hoheren temperaturen [J]. Allgem Anorg Chem, 1927, 1: 1−12. (in German)
[43] GINSTLING A M, BROUNSHTEIN B I. Concerning the diffusion kinetics of reactions in spherical particles [J]. Journal of Applied Chemistry, 1950, 23: 1327−1338.
[44] LEVENSPIEL O. Chemical reaction engineering [M]. 2nd ed. New York: John Wiley & Sons, Inc, 1972.
[45] PAIK J G, LEE M J, HYUN S H. Reaction kinetics and formation mechanism of magnesium ferrites [J]. Thermochimica Acta, 2005, 425(1−2): 131−136.

熔融 Al−Cr−V−B 合金中 CrB_2 和 VB_2 形成的热力学和动力学分析

A. KHALIQ[1,2], H. T. ALI[3], M. YUSUF[4]

1. Department of Mechanical Engineering, College of Engineering, University of Ha'il, Kingdom of Saudi Arabia;
2. School of Engineering, RMIT University, Melbourne, VIC 3000, Australia;
3. Department of Mechanical Engineering, College of Engineering, Taif University, P. O. Box 11099, Taif 21944, Kingdom of Saudi Arabia;
4. Department of Clinical Pharmacy, College of Pharmacy, Taif University, P. O. Box 11099, Taif 21944, Kingdom of Saudi Arabia

摘　要：熔体中的铬(Cr)、钒(V)等过渡金属杂质会降低冶炼级铝(Al)的电导率。这些杂质可与含硼(B)物质发生原位反应形成硼化物，因此可以通过硼处理除去熔体中的杂质。然而，对于冶炼级铝熔体的除铬尚不清楚。文献中关于在其他过渡金属(V，Ti，Zr，Fe)存在的条件下，往熔融铝中加入 Al−B 母合金时硼化铬(CrB_2)的形成存在分歧。本研究在 1023 K 下往铝合金熔体中加入 Al−B(AlB_{12})母合金，探讨 Al−0.50%Cr−0.50%V(质量分数)合金除铬的机理。结果表明，在 1023 K 下，无法通过形成稳定的硼化物从熔融的 Al−0.50%Cr−0.50%V 合金中除铬。在熔融铝的硼处理过程中，熔体中过量的 B 优先形成硼化铝(AlB_2)，而不是 CrB_2。从熔融 Al−0.50%Cr−0.50%V 合金中除钒的动力学研究表明，初期反应阶段由[B]/[V]的液相传质控制，传质系数(k_m)为 9.6×10^{-4} m/s；后期反应阶段受[B]/[V]通过硼化物(VB_2)环的扩散控制。因此，建议研究从熔融铝中除铬的替代方法。

关键词：硼处理；铝；CrB_2；VB_2；热力学；动力学

(Edited by Wei-ping CHEN)